ALBERT-LUDWIG UNIVERSITY FREIBURG
Institute of Computer Science
Chair for Pattern Recognition and Image Processing

Tile-based Lucy-Richardson Deconvolution Modeling a Spatially-Varying PSF for Fast Multiview Fusion of Microscopical Images

Maja Temerinac-Ott

Technical Report 260

August 2010

Chair for Pattern Recognition and Image Processing
University of Freiburg

Tile-based Lucy-Richardson Deconvolution Modeling a Spatially-Varying PSF for Fast Multiview Fusion of Microscopical Images

Maja Temerinac-Ott

University of Freiburg
Institute of Computer Science
Chair for Pattern Recognition and Image Processing
Georges-Koehler-Allee Geb. 052
79110 Freiburg, Germany

Telephone +49 761 203 8275, Fax +49 761 203 8262
e-mail: temerina@informatik.uni-freiburg.de

Technical Report 260

August 2010

Abstract

A framework for fast multiview fusion of Single Plane Illumination Microscopy (SPIM) images based on a spatially-variant point spread function (PSF) model recorded using fluorescent point markers (beads) inserted into the surrounding medium is presented. The beads are used for the registration of the images as well as for the estimation of the spatially-varying PSF function.

A new fusion algorithm based on regularized Lucy-Richardson deconvolution and the Overlap-Save method (LROS-TV) is presented and tested on SPIM images.

Our framework proposes a method of decomposing the image into small packages thus saving memory space and allowing for parallel processing. As to our knowledge this is the first framework allowing modeling of spatially-variant PSF functions for SPIM images.

1 Introduction

Single Plane Illumination Microscopy (SPIM) [3] is a powerful tool for recording deep inside live embryos. It combines the advantages of widefield and confocal microscopy to produce images of high resolution of e.g. zebrafish embryos. SPIM is fast since it records the whole image plane at once (like the widefield) however it only collects light from one plane which keeps the scattering small. The quality of the images is slightly worse than images recorded with confocal microscopy. The main advantage of the SPIM however is its mounting technique inside a gel cylinder which makes the objects to be recorded easily movable. Thus one is able to rotate the gel cylinder easily and take images from the same object from different views. In this way one can compensate for absorption and scattering by just taking another image from a slightly different angle. The resulting recordings comprise a number of different views of the same object which need to be 1. registered and 2. fused.

Many solutions for the post processing of the SPIM images have already been proposed ([10], [8], [4]) and solutions for higher resolved images have been sought on both hardware and software sides. Only a combination of high quality hardware and specialized algorithms for this hardware will lead to good results.

In this work we would like to propose a new framework for the SPIM post processing. Our goal is to keep memory space and computation time as low as possible in order to make the technology approachable for everyday use in the lab. After registration, the images are decomposed in small packages, that can be processed independently from each other. The multiview-fusion is conducting using Overlap-Save deconvolution and the Lucy-Richardson algorithm. This result in three advantages over already existing methods: 1. A spatially-variant PSF can be modeled, 2. Only small amounts of memory is used and 3. the algorithm can be performed using parallel computation.

2 Related Methods

There have already been developed complete solutions for SPIM reconstruction over the years.

In the beginning ([10]) the registration was performed only using the gray value image of the recorded images. The registration based on gray values only has two major drawbacks: 1. its computation time is very high for large images and 2. the verification of the registration results on a pixel bases is very difficult, since one does not know the original shape of the recorded objects. This two drawbacks were overcome in [8] by inserting fluorescent point markers (beads) into the surrounding medium of the object. The shape and the size of the beads is previously known, so that there positions can be easily extracted. Only the beads are used to compute the transformation parameters which keeps the recording time very low. The precision of the registration can then be exactly expressed as the distance between corresponding beads.

For the fusion there are two possible solutions: 1. to combine the gray values or 2. multi-view deconvolution of several stacks. The first solution can be done by simple operators as maximum, average or by more elaborate methods such as weighted blending [8]. The results of this first kind of methods can look optically very nice, however they do not account for deformations introduced by the point spread function (PSF). This has the major drawback of wrong metrics of the objects, e.g. the size of the cells: Round cells will not have the same radius in all directions. The first kind of methods however is very fast.

The second kind of methods which are based on deconvolution are more computation time consuming. They depend on the correct estimation of the PSF and can produce artifacts which are optically not very pleasant. Also, they are more time consuming and if performed on the whole image require more memory. So far ([10], [5]) one PSF was assumed per view. In [5] the Lucy-Richardson algorithm was modified for multiview deconvolution.

In this work we will extend this solution by accounting also for the space-variance of the PSF which is measured using beads. To assume a spatially-variant PSF for the whole light sheet is not correct since the light sheet has not the same thickness overall in space. Thus using a spatially-variant PSF better describes the image formation process.

3 Overview of the Framework

Our general framwork is presented in Fig. 1. Fist a biological sample is recorded from different angles using single plane illumination microscopy. Second the bead positions are computed using morphological operators. Third the beads are used for the registration of the different views. Fourth the point spread function of the beads is estimated

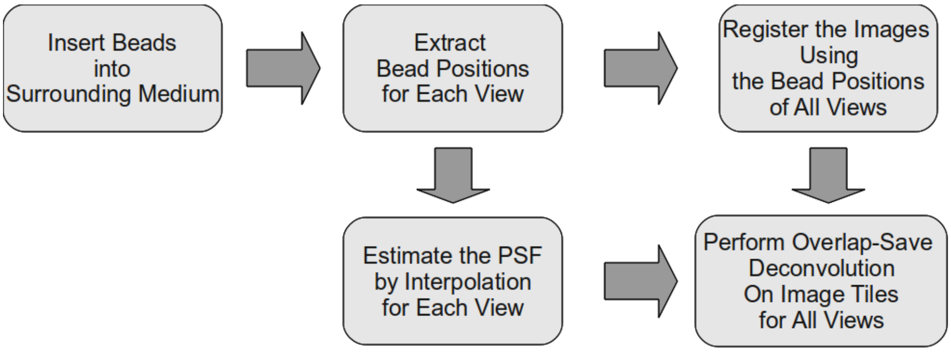

Figure 1: The general framework for the tile-based multiview fusion.

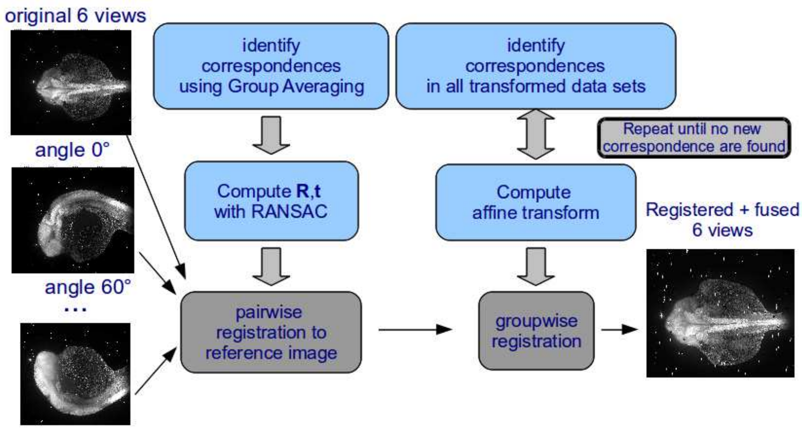

Figure 2: Groupwise-Registration of SPIM images using the bead positions.

at the bead positions and interpolated in regions where no beads were present. Finally, using Overlap-Save method and the Lucy-Richardson algorithm the image is deconvolved and fused at the same time.

3.1 Extraction of the Beads

The bead positions are computed by thresholding the image thus separating foreground and background pixels. The threshold is computed using the Otsu method or by manual selection. Than the image is smoothed by a Gaussian filter and local maxima are computed. The local maxima are potential candidates for bead positions. Our goal is to select beads which are outside the recorded object. Thus we need to compute all the voxels which belong to the recorded object. This is done by binarizing the original image using an appropriate threshold. Afterwards the largest component of the image is computed using connected component labeling. All the local maxima which are not part of the largest component are taken as bead coordinates.

3.2 Registration of the Beads

Local descriptors based on Group Averaging [11] are extracted in order to find corresponding beads between the views. Then the found correspondences are used to perform groupwize registration and finally compute an affine transform (Fig. 2).

3.3 Extraction of the PSF

We extract a window of size r around each position and save it as a PSF estimate. The PSF estimates are normalize to have the energy one. We will discard the PSF estimates if the bead coordinates are too close (Fig. 3).

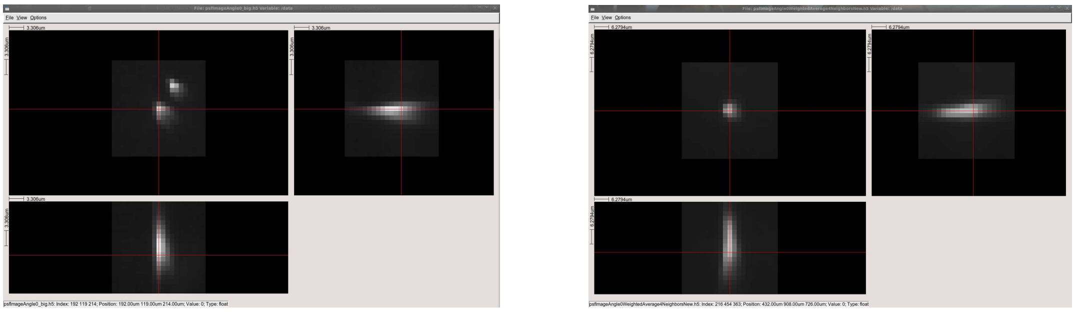

(a) (b)

Figure 3: Orthoview of a (a) Bead which is too close to a second Bead and (b) a well segmented PSF.

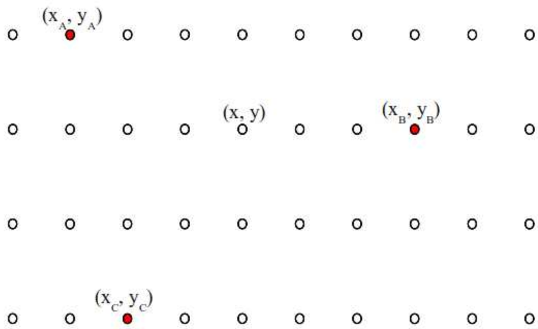

Figure 4: The PSF at position (x, y) is interpolated using beads at position A, B, C.

3.4 Interpolation of the PSF

So far we use nearest neighbor and linear interpolation to estimate the PSF function at a random position. The basic assumption for the interpolation algorithm is a smooth PSF change. Consider Fig. 4: If the PSF functions in three points (A, B, C) are known as h_A, h_B, h_C, the we can interpolate the PSF function for point (x, y) as:

$$H(n, k) = \frac{d_B d_C h_A(n, k) + d_A d_C h_B(n, k) + d_A d_B h_C(n, k)}{d_B d_C + d_A d_C + d_A d_B} \tag{1}$$

with distances of the point (x, y) to the three points A, B, C:

$$d_A = \sqrt{(}(x - x_A^2) + y - y_A^2)) \tag{2}$$

and d_B, d_C respectively.

3.5 Spatially-variant deconvolution

The original image is divided into tiles of size $s \times s$ and deconvolution is performed for each tile individually. The regularized Lucy-Richardson algorithm for multiple views is is used for deconvolution. The single tiles are stitched together using the Overlap-Save method.

4 Lucy-Richardson Deconvolution

In [6], [9] Lucy and Richardson develop an iterative expectation maximization deconvolution algorithm based on a Bayesian framework:

$$p(X|Y) = p(Y|X) \cdot \frac{p(X)}{p(Y)}, \tag{3}$$

where $p(Y|X)$ is the likelihood probability, $p(X|Y)$ the posteriori probability, and $p(X)$ a prior model of the image.

In [2] a formulation of the likelihood probability for image statistics described by a Poisson process is given as:

$$p(Y|X) = \prod_{\mathbf{v}} \frac{[H * X(\mathbf{v})]^{Y(\mathbf{v})} \cdot e^{-(H*X)(\mathbf{v})}}{Y(\mathbf{v})!}, \tag{4}$$

where $X, Y, H : \mathbb{R}^3 \mapsto \mathbb{R}, \mathbf{v} \in \mathbb{R}^3$. The likelihood probability Eq. (4) is maximized by minimizing the negative log likelihood:

$$-\log p(Y|X) = \int_{\mathbf{v}} [(H * X)(\mathbf{v}) - Y(\mathbf{v}) \log(H * X)(\mathbf{v}) + \log(Y(\mathbf{v})!)] d\mathbf{v}, \tag{5}$$

where the term $\log(Y(\mathbf{v})!)$ in Eq. (4) is a constant relative to X. Thus it is enough to minimize the functional $J(X)$ defined as:

$$J(X) = \int_{\mathbf{v}} [(H * X)(\mathbf{v}) - Y(\mathbf{v}) \log(H * X)(\mathbf{v}) d\mathbf{v}. \tag{6}$$

In order to compute the derivative of the functional J, we add a small perturbation $\rho X'$ to the original image X and approximate the change of the functional:

$$\begin{aligned}
J(X + \rho X') &= \int_{\mathbf{v}} [(H * (X + \rho X'))(\mathbf{v}) - Y(\mathbf{v}) \log\left((H * (X + \rho X'))(\mathbf{v})\right)] d\mathbf{v} && (7)\\
&= \int_{\mathbf{v}} [(H * X)(\mathbf{v}) + \rho (H * X')(\mathbf{v}) - Y(\mathbf{v}) \cdot \log\left((H * X)(\mathbf{v}) \cdot (1 + \rho \frac{H * X'}{H * X})(\mathbf{v})\right)] d\mathbf{v} && (8)\\
&\simeq \int_{\mathbf{v}} [(H * X)(\mathbf{v}) + \rho (H * X')(\mathbf{v}) - Y(\mathbf{v}) \cdot \log((H * X)(\mathbf{v})) - \rho Y(\mathbf{v}) \cdot \frac{H * X'}{H * X}(\mathbf{v})] d\mathbf{v} && (9)\\
&= J(x) + \rho \int_{\mathbf{v}} [(H * X')(\mathbf{v}) - Y(\mathbf{v}) \frac{H * X'}{H * X}(\mathbf{v})] d\mathbf{v}. && (10)
\end{aligned}$$

The derivative is obtained using the scalar product defined by $\langle f, g \rangle = \int_{\mathbf{v}} (fg)(\mathbf{v}) d\mathbf{v}$:

$$\langle \frac{\partial J(X)}{\partial X}, \rho X' \rangle = \lim_{p \to X^+} \frac{J(X + \rho X') - J(X)}{\rho}. \tag{11}$$

By writing Eq. (10) as scalar product and applying basic rules to the scalar product we obtain:

$$\begin{aligned}
\int_{\mathbf{v}} (H * X')(\mathbf{v}) - Y(\mathbf{v}) \frac{H * X'}{H * X}(\mathbf{v}) d\mathbf{v} &= \langle 1, H * X' \rangle - \langle \frac{Y}{H * X}, H * X' \rangle && (12)\\
&= \langle H^*, X' \rangle - \langle \frac{Y}{H * X} * H^*, X' \rangle && (13)\\
&= \int_{\mathbf{v}} X'(\mathbf{v}) \left(H^* - \left[H^* * \left(\frac{Y}{H * X} \right) \right] \right) (\mathbf{v}) d\mathbf{v}, && (14)
\end{aligned}$$

where H^* is the adjoint of the operator H and in case of the PSF $H^*(\mathbf{v}) = H^*(-\mathbf{v})$. The derivative of the functional can then be expressed as:

$$\nabla J(X(\mathbf{v})) = H(-\mathbf{v}) * \left[1 - \frac{Y(\mathbf{v})}{(H * X)(\mathbf{v})} \right] \tag{15}$$

After setting the derivative to zero ($\nabla J(X) = 0$) we obtain:

$$\int_{\mathbf{v}} H(-\mathbf{v}) d\mathbf{v} - H(-\mathbf{v}) \cdot \frac{Y(\mathbf{v})}{(H * X)}(\mathbf{v}) = 0. \tag{16}$$

Since the PSF has the energy one, we obtain finally:

$$H(-\mathbf{v}) * \frac{Y(\mathbf{v})}{(H * X)}(\mathbf{v}) = 1. \tag{17}$$

By assuming that at convergence the ratio $\frac{X^{p+1}}{X^p}$ is 1, we define the iteration steps as:

$$\hat{X}^{p+1}(\mathbf{v}) = \hat{X}^p(\mathbf{v}) \cdot \left[H(-\mathbf{v}) * \frac{Y(\mathbf{v})}{(H * \hat{X}^p)}(\mathbf{v}) \right] \tag{18}$$

$$= \hat{X}^p(\mathbf{v}) \cdot \left[H(-\mathbf{v}) * \frac{Y(\mathbf{v})}{S^p(\mathbf{v})} \right] \tag{19}$$

$$= \hat{X}^p(\mathbf{v}) \cdot C^p(\mathbf{v}), \tag{20}$$

where $\hat{X}^p$ is the current estimate of the original image X at iteration p and S is the simulated image using the PSF H. Thus, in each iteration step p the former estimate of the original image $\hat{X}$ is multiplied by the correction factor C:

$$C^p(\mathbf{v}) = H(-\mathbf{v}) * \frac{Y(\mathbf{v})}{S^p(\mathbf{v})}. \tag{21}$$

The LR algorithm is never negative as long as the initial estimate was not negative. For noisy images, the LR algorithm amplifies the noise and thus regularization is required to obtain a smooth solution. The algorithm converges slowly to the optimal solution and then diverges again. The stop criterion can either be a fixed number of iteration steps or the difference between two estimates $\hat{X}_p$ and $\hat{X}_{p+1}$.

4.1 Multiview Lucy-Richardson Algorithm

The original Lucy-Richardson algorithm is extended in [5] for multiview fusion. For N recordings $(Y_1, ..., Y_N)$ and the corresponding PSFs $(P_1, ..., P_N)$, the correction factor C is computed for each image Y_i individually. The final correction factor is than computed as an average of the individual correction factors:

$$C^p = \frac{1}{N} \sum_{i=1}^{N} C_i^p \tag{22}$$

$$C_i^p = H_i(-\mathbf{v}) * \frac{Y_i(\mathbf{v})}{S_i^p(\mathbf{v})} \tag{23}$$

$$S_i^p(\mathbf{v}) = H_i * \hat{X}(\mathbf{v}). \tag{24}$$

The old estimate of X is then multiplied by this combined correction factor. So the original algorithm of Lucy-Richardson stays the same except of the computation of the combined correction factor.

As an initial estimate for the original image, the average of all recorded views is taken:

$$\hat{X}^0 = \frac{1}{N} \sum_{i=1}^{N} Y_i^p. \tag{25}$$

4.2 Regularization of the Lucy-Richardson Algorithm

In [1] Total Variation (TV) is used for regularization of the Lucy-Richardson algorithm. Total variation preserves the borders and suppresses the noise. When extremized it will produce cartoon like structures. The multiview fusion algorithm presented in the previous section is regularized by adding the TV term to the function J, resulting in the function J_{TV}:

$$J_{TV} = J(X\mathbf{v}) + \lambda \int_{\mathbf{v}} |\nabla X(\mathbf{v})| d\mathbf{v} \tag{26}$$

In the above algorithm this results in dividing the image $\hat{X}^p$ in Eq. (20) by a factor before applying the correction factor:

$$\hat{X}_{p+1}(\mathbf{v}) = \frac{\hat{X}^p(\mathbf{v})}{1 - \lambda \text{div}\left(\frac{\nabla \hat{X}^p(\mathbf{v})}{|\nabla \hat{X}^p(\mathbf{v})|}\right)} \cdot C^p(\mathbf{v}) \tag{27}$$

For the derivation of this iteration step we refer to [1].

5 Overlap-Save Method

Assume the original image is noted by $X : \mathbb{R}^2 \mapsto \mathbb{R}$, the PSF by $H : \mathbb{R}^2 \mapsto \mathbb{R}$ and the convolved image by $Y : \mathbb{R}^2 \mapsto \mathbb{R}$. Then, the convolution of H with X is written as:

$$Y = H * X, \tag{28}$$

where $*$ denotes the convolution operation.

For the tile-based deconvolution the convolved image is partitioned in tiles of size s, where s is an even number. The size of the PSF function H is r where r is an uneven number. We assume that $s + r = 2^k$, which will later be important when we perform the block-wise Fast Fourier Transform (FFT).

The unknown result Y is partitioned as:

$$\begin{bmatrix} Y_{11} & Y_{12} & \dots & Y_{1n} \\ Y_{21} & Y_{22} & \dots & Y_{2n} \\ \vdots & \vdots & & \vdots \\ Y_{n1} & Y_{n2} & \dots & Y_{nn} \end{bmatrix}. \tag{29}$$

Than the convolution algorithm is performed as ([7]):

Algorithm 1: Overlap-Save algorithm

for $i = 1$ to n **do**
  for $j = 1$ to n **do**
    1. Extract extended region $X_{ij}^{(r+s)}$ from X.
    2. Obtain $H^{(r+s)}$ by padding with zeros.
    3. Compute the convolved tile: $Y_{ij}^{(r+s)} = \texttt{ifft2}(\texttt{sfft2}(H^{(r+s)} \circ \texttt{fft2}(X_{ij}^{(r+s)})$
    4. Extract Y_{ij} from $Y_{ij}^{(r+s)}$ and save into Y.
  end for
end for

Herby $\circ$ denotes the element-wise multiplication, $\texttt{fft2}(.)$ stands for the FFT for two dimensional images and $\texttt{ifft2}(.)$ for the inverse FFT. $\texttt{sfft2}(.)$ denotes the 2D FFT of a shifted array. $Y_{ij}^{(r+s)}$ denotes the tile Y_{ij} of size $s \times s$ padded by its neighboring pixels in the neighborhood r:

$$Y_{ij}^{(r+s)} = \begin{bmatrix} \times & \times & \times \\ \times & Y_{ij} & \times \\ \times & \times & \times \end{bmatrix}. \tag{30}$$

The tile-based deconvolution algorithm is performed in the same manor except that in step 4 of Alg. 1 a deconvolution is performed. In this way spatially-variant PSF functions can be modeled.

6 Lucy-Richardson Overlap-Save Multiview Method Using Total Variation (LRMOS-TV)

The combined algorithm (LRMOS-TV) for three dimensional images is than:

for $m = 1$ to n **do**
  for $n = 1$ to n **do**
    for $k = 1$ to n **do**
      1. Extract extended region $R_i = Y_{mnk}^{(r+s)}$ from Y_i for each view i.
      2. Obtain $H_i = H_{m,n,k}^{(r+s)}$ by padding with zeros for each view i.
      3. Compute the initial estimate $\hat{X}^0 = \frac{1}{N}\sum_{i=1}^{N} R_i^p$
      4. Iterate $\hat{X}_{m,n,k}^{p+1}(\mathbf{v}) = \frac{\hat{X}_{m,n,k}^{p}(\mathbf{v})}{1-\lambda \mathrm{div}\left(\frac{\nabla \hat{X}_{m,n,k}^{p}(\mathbf{v})}{|\nabla \hat{X}_{m,n,k}^{p}(\mathbf{v})|}\right)} \cdot C^p(\mathbf{v})$
      5. Extract $\hat{X}_{mnk}$ from $\hat{X}_{mnk}^{(r+s)}$ and save into $\hat{X}$.
    end for
  end for
end for

7 Experiments on 2D Images

The original *Lena* image of size $(M \times M)$, $M = 512$ is convolved using a spatially-variant PSF and deconvolved using the Overlap-Save method (Fig. 5).

The spatially-variant PSF function at point (i, j) is obtained by rotating a basic PSF H_0 depending on its distance to the center of the image in order to obtain a smooth spatially varying PSF functions (Fig. 5 (b)):

$$d = \sqrt{(i - (N/2))^2 + (j - (N/2))^2} \tag{31}$$

$$H_{i,j} = R(d/(N/2))H_0, \tag{32}$$

where $R(\alpha)$ rotates a 2D matrix for angle α around its center.

The basic PSF function H_0 is a Gaussian function of the form:

$$H_0(x + \mathrm{floor}(r/2), y + \mathrm{floor}(r/2)) = \exp(-(x^2/(2\sigma_1^2) + (y^2/(2\sigma_2^2))), \tag{33}$$

where $\sigma_1 = 4$, $\sigma_2 = 2$ and $r = 21$.

The convolution (Fig. 5 (c))is performed using the Overlap-Save algorithm Alg. 1 The deconvolution (Fig. 5 (d)) is performed using the Lucy-Richardson algorithm (Eq. 27). 20 iterations are performed and $\lambda = 0.000006$.

8 Results on SPIM images

Recordings of a 24h zebrafish recorded from six views using SPIM are fused using the proposed framework. The zebrafish is stained with Sytox and embedded in a Glycerol solution filled with latex-fluorophore beads of $1\mu m$ diameter. The beads are very bright when compared with the brightness of the zebrafish. A W-Plan -Apochromat (20x/1.0 M27) lens is used and each view is illuminated from two sides resulting in two images per view. The two images are fused by averaging to produce a more evenly illuminated image. The sample is rotated for 60° around the y-axis. The resulting image has a size of (751×1040) voxels of size $(1\mu m \times 1.10897\mu m \times 1.10897\mu m)$ for the (z, y, x) dimensions respectively. All the computations are performed on images scaled to the isotropic voxel size $(2\mu m \times 2\mu m \times 2\mu m)$.

8.1 Parameters for the Deconvolution

For the Lucy-Richardson algorithm we use PSF of size $r = 11$ and padded tiles of size 64. Five iterations of the multiview Lucy-Richardson algorithm are performed for each tile. The regularization parameter $\lambda = 0.0001$.

The computation is performed with Matlab (R2009a) on a 4x QuadCore Xeon X7350 2.93GHz CPU. The computation time is 45 minutes for the Fusion of the six views. So far only the convolution is implemented as a

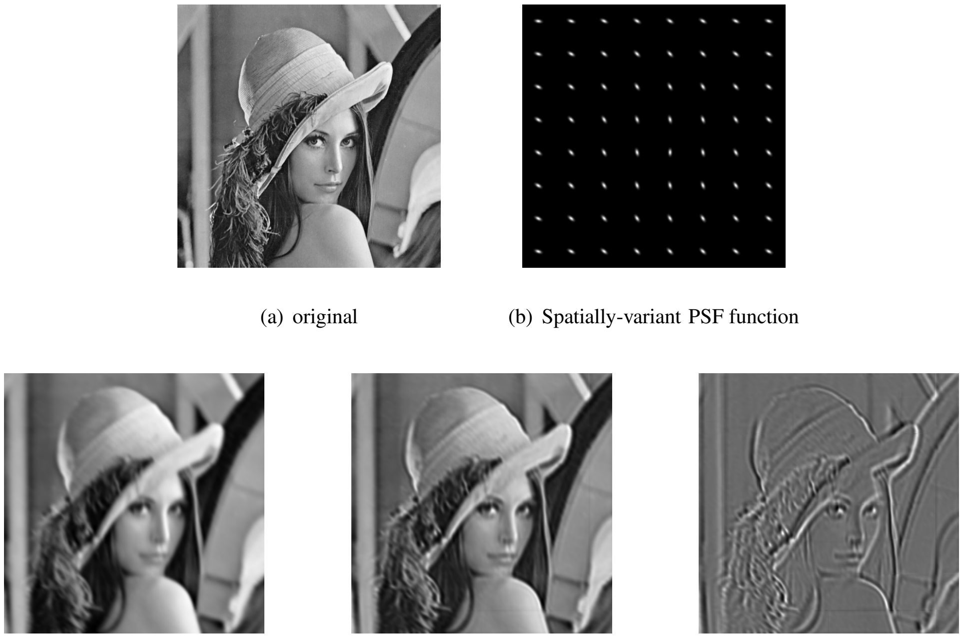

(a) original

(b) Spatially-variant PSF function

(c) Convolved Image

(d) Deconvolved Image

(e) Difference Convolved - Deconvolved

Figure 5: Tile-based deconvolution of the Lena image using Overlap-Save method and the Lucy-Richardson algorithm for deconvolution.

FFT and thus parallelized. The tiles are processed sequentially. In future we plan to redistribute the processing of the single tiles to several computers.

8.2 Comparison to Average and Maximum Selection

After registration (Fig. 2), the registered images are fused by Averaging, Maximum selection and the Overlap-Save proposed LRMOS-TV algorithm. In Tab. 1 the main properties of the three fusion methods are presented. The Averaging produces Round Beads and suppresses noise (Fig. 6), however the small structures (e.g. cells) are blurred and cannot be separated any more (Fig. 7). The Maximum selection enhances the original structures and at the same time the noise, thus adding new structures to the image. This property is not desirable at all for the further analysis of the data. The LRMOS-TV algorithm preserves the cell structures while at the same time suppressing noise. The bead retains its original spherical structure and is no longer star shaped.

In Fig.7(c) the tile border is visible at the lower part of the image. The borders become visible if neighboring PSF functions are not smooth enough or if the number of iterations is to large. The TV parameter λ can exaggerate edges as well and thus lead to visible borders. The choice of the right parameters will be subject to further research.

LRMOS-TV	MAX	Average
good contrast	good contrast	bad contrast
round beads	star shaped beads	round beads
suppresses noise	enhances noise	suppresses noise

Table 1: Properties of Average, MAX and Lucy-Richardson fusion.

8.3 Comparison with Blending

The Fiji-plugin as described in [8] was used for the fusion of the six views and the results can be compared in Fig. 8. Especially in the eye region the structures which are averaged during blending are preserved using the

LRMOS-TV fusion.

9 Conclusions

A new framework for the fusion of SPIM images was presented based on the Overlap-Save regularized Lucy-Richardson deconvolution. The LRMOS-TV algorithm can be easily implemented in Matlab and produces better results than the blending. For further processing e.g. segmentation the LRMOS-TV deconvolution can be very helpful since it enhances the structure's border.

Further topics of research will include additional regularization strategies (e.g. Tikhonov-Miller) as well as the optimal number of iteration steps. Furthermore we would like to develop a parametric model of the PSF along the light sheet.

10 Acknowledgements

This study was supported by the Excellence Initiative of the German Federal Governments (EXC 294) and the SFB 592.

References

[1] N. Dey, L. Blanc-Feraud, C. Zimmer, P. Roux, Z. Kam, J.-C. Olivio-Marin, and J. Zerubia. 3d microscopy deconvolution using richardson-lucy algorithm with total variation regularization. Technical report, INRIA, 2004.

[2] T. Hebert and R. Leahy. A generalized em algorithm for 3-d bayesian reconstruction from poisson data using gibbs priors. *Medical Imaging, IEEE Transactions on*, 8(2):194 –202, jun 1989.

[3] J. Huisken, J. Swoger, F. D. Bene, J. Wittbrodt, and E. H. K. Stelzer. Optical sectioning deep inside live embryos by selective plane illumination microscopy. *SCIENCE*, 305:1007–1009, August 2004.

[4] P. J. Keller, A. D. Schmidt, A. Santella, K. Khairy, Z. Bao, J. Wittbrodt, and E. H. K. Stelzer. Fast, high-contrast imaging of animal development with scanned light sheetbased structured-illumination microscopy. *Nature Methods*, 7:637–42, 2010.

[5] U. Krzic. *Multiple-view microscopy with light-sheet based fluorescence microscope*. PhD thesis, Rupert-Carola University of Heidelberg, 2009.

[6] L. B. Lucy. An iterative technique for the rectification of observed distributions. *The Astronomical Journal*, 79(6):745–754, 1974.

[7] J. G. Nagy and D. P. O'Leary. Fast iterative image restoration with a spatially-varying psf. Technical Report 3810, University of MAryland, 1998.

[8] S. Preibisch, S. Saalfeld, J. Schindelin, and P. Tomancak. Software for bead-based registration of selective plane illumination microscopy data. *Nature Methods*, 7:418–419, 2010.

[9] W. H. Richardson. Bayesian-based iterative method of image restoration. *Journal of the Optical Society of America*, 62(1):55–59, 1972.

[10] J. Swoger, P. Verveer, K. Greger, J. Huisken, and E. H. K. Stelzer. Multi-view image fusion improves resolution in three-dimensional microscopy. *Opt. Express*, 15(13):8029–8042, 2007.

[11] M. Temerinac-Ott, M. Keuper, and H. Burkhardt. Evaluation of a new point clouds registration method based on group averaging features. In *Proceedings of 20th International Conference on Pattern Recognition (ICPR 2010)*, Istanbul, Turkey, 2010. (accepted).

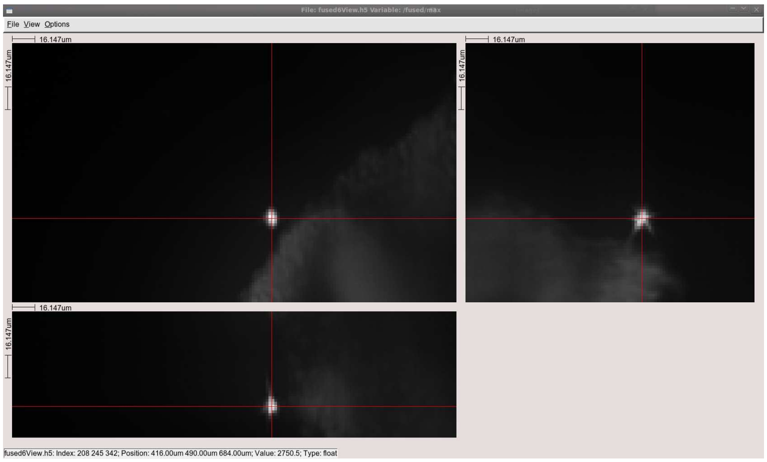

(a) MAX fusion

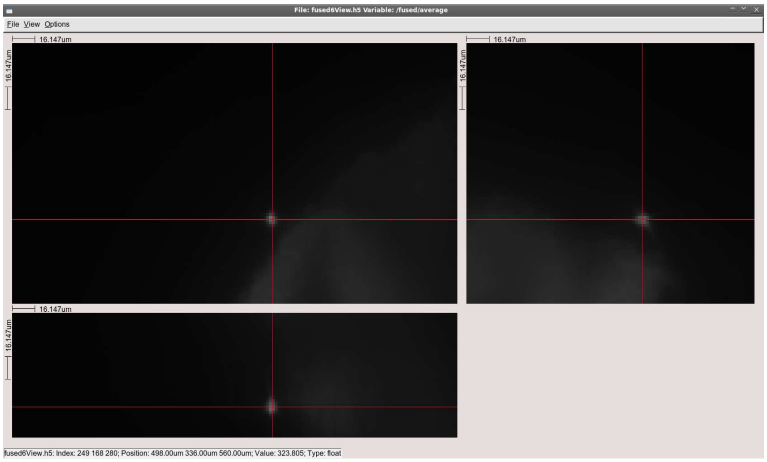

(b) Average fusion

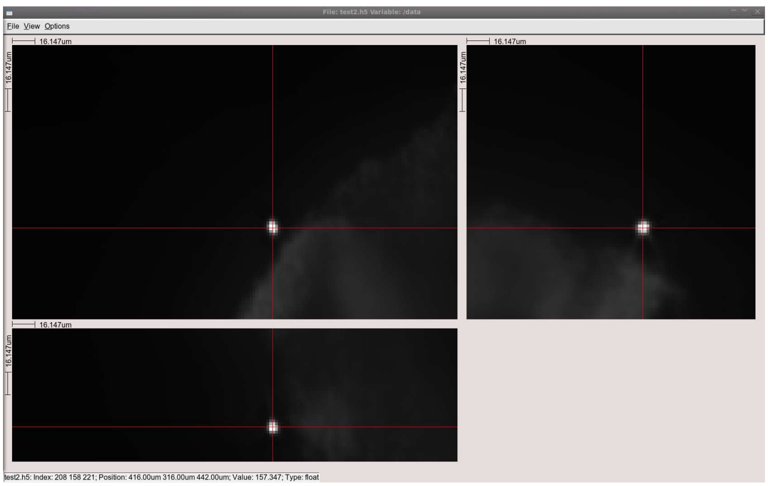

(c) LRMOS-TV

Figure 6: MAX, Average and LRMOS-TV fusion of one bead.

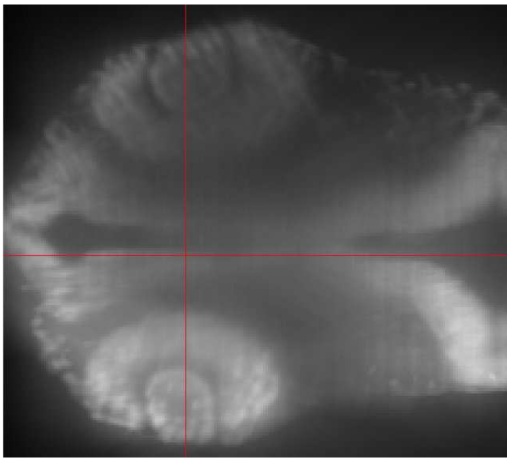

(a) MAX fusion

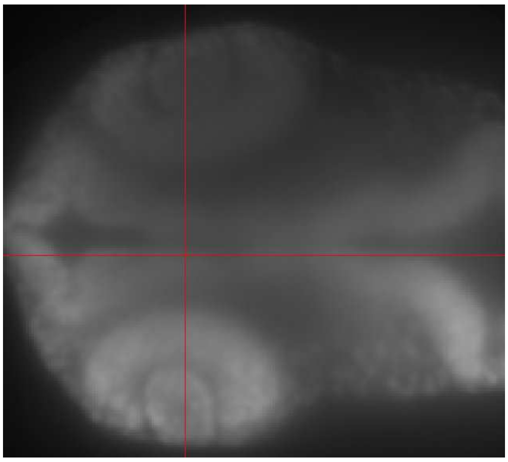

(b) Average fusion

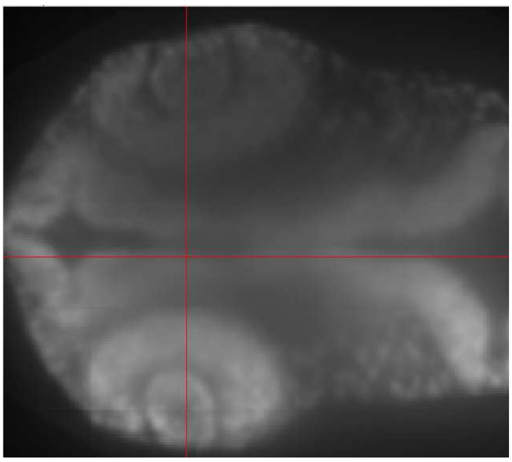

(c) LRMOS-TV

Figure 7: MAX, Average and Lucy-Richardson deconvolved head of the zebrafish.

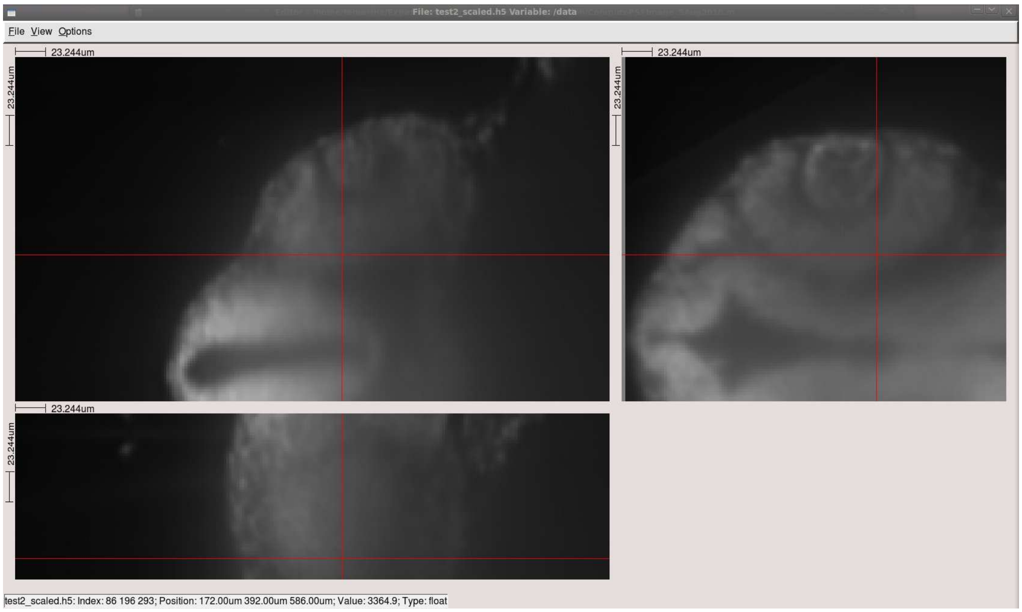

(a) LRMOS-TV

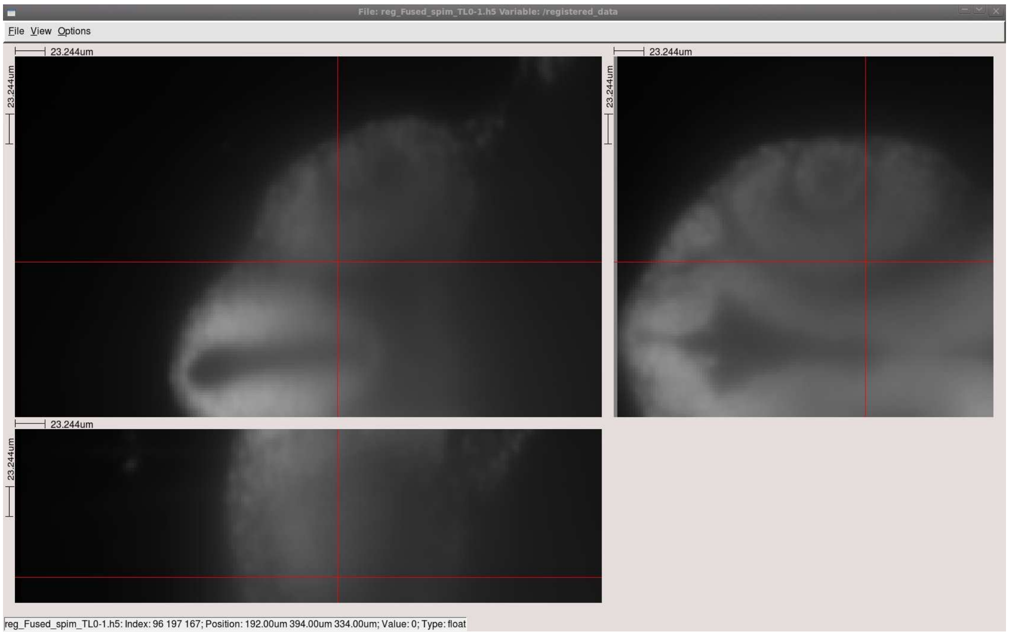

(b) Blending [8]

Figure 8: Comparison of the LRMOS-TV fusion and blending fusion [8].